Biometrics, 2024, 80(1), ujad019
https://doi.org/10.1093/biomtc/ujad019
Biometric Methodology

A flexible framework for spatial capture-recapture with unknown identities

Paul van Dam-Bates [1,*], Michail Papathomas [1], Ben C. Stevenson [2], Rachel M. Fewster [2], Daniel Turek [3], Frances E.C. Stewart [4], David L. Borchers [1,5]

[1]School of Mathematics and Statistics, University of St Andrews, St Andrews, Fife, KY16 9LZ, United Kingdom, [2]Department of Statistics, University of Auckland, Auckland, 1010, New Zealand, [3]Department of Mathematics and Statistics, Williams College, Williamstown, 01267, United States, [4]Department of Biology, Wilfrid Laurier University, Waterloo, N2L 3C5, Canada, [5]Centre for Statistics in Ecology, Environment and Conservation, Department of Statistical Sciences, University of Cape Town, Private Bag 7700, Rondebosch, South Africa

[*]Corresponding author: Paul van Dam-Bates, The Observatory, Buchanan Gardens, St. Andrews, Fife, KY16 9LZ, United Kingdom (paul.vandambates@gmail.com).

ABSTRACT

Camera traps or acoustic recorders are often used to sample wildlife populations. When animals can be individually identified, these data can be used with spatial capture-recapture (SCR) methods to assess populations. However, obtaining animal identities is often labor-intensive and not always possible for all detected animals. To address this problem, we formulate SCR, including acoustic SCR, as a marked Poisson process, comprising a single counting process for the detections of all animals and a mark distribution for what is observed (eg, animal identity, detector location). The counting process applies equally when it is animals appearing in front of camera traps and when vocalizations are captured by microphones, although the definition of a mark changes. When animals cannot be uniquely identified, the observed marks arise from a mixture of mark distributions defined by the animal activity centers and additional characteristics. Our method generalizes existing latent identity SCR models and provides an integrated framework that includes acoustic SCR. We apply our method to estimate density from a camera trap study of fisher (*Pekania pennanti*) and an acoustic survey of Cape Peninsula moss frog (*Arthroleptella lightfooti*). We also test it through simulation. We find latent identity SCR with additional marks such as sex or time of arrival to be a reliable method for estimating animal density.

KEYWORDS: acoustic recorders; camera traps; marked Poisson processes; mixture model; spatial clustering.

1 INTRODUCTION

Estimates of animal density, the number of individuals per unit area, are critically important for understanding ecological processes affecting wildlife management. Spatial capture-recapture (SCR) can be used to estimate animal density from detections of animals at multiple points in space, when animal identities are known (Efford, 2004; Borchers and Efford, 2008; Royle et al., 2013). In the case of acoustic SCR (ASCR), detections are of animal vocalizations, not of animals themselves. Because it is often feasible to identify which detectors recorded each vocalization (or cue), but not the animal that vocalized, ASCR generally estimates vocalization density (Stevenson et al., 2015). When individual identification is difficult or impossible, there is a need for methods that can accommodate unobserved (latent) identities. We refer to these methods as "latent ID" models.

We are motivated by 2 datasets: a camera trap study of fisher (*Pekania pennanti*) (Burgar et al., 2018) and an acoustic survey of Cape Peninsula moss frog (*Arthroleptella lightfooti*) (Stevenson et al., 2021). In the fisher example, a portion of the detections can be identified as male or female, as well as collared or uncollared, due to a parallel telemetry study. Using the collars to inform animal identity results in a specific type of spatial mark-resight problem with batch marking, as the collars are not uniquely identifying (Cowen et al., 2017). The collars were also removed during the camera trap study, adding a unique challenge to this dataset that has not been explored in the literature.

Latent ID SCR literature consists mainly of extensions to the spatial count (SC) model developed by Chandler and Royle (2013) that models the aggregated counts at each detector of the latent individuals. For cases when there are partially identifying features (ie, pelage or sex), Augustine et al. (2018) took the approach of modeling the individual detections in what is known as spatial partial identity models (SPIMs). Both SC and SPIM are extensions of SCR that make inference by using the spatial location of each animal to sample from the latent capture history in a Markov Chain Monte Carlo (MCMC) framework. The SC approach models the count of detections at each trap across all individuals, and the latent capture history is then sampled by allocating detections to the unobserved animals or by marginalizing over all possible identities. Chandler and Royle (2013) showed that for reliable inference, it is necessary to have either strong prior knowledge of animal home range or a proportion of the population with fully known identities. Spatial capture-recapture is then applied to the known ID portion, and the SC model is applied to the additional latent ID counts (Sollmann

Received: November 18, 2022; Revised: October 30, 2023; Accepted: November 22, 2023

et al., 2013; Rich et al., 2014; Alonso et al., 2015; Whittington et al., 2018). SC models have also been used when animal identity is missing randomly, such as from poor picture quality (Jiménez et al., 2021).

Instead of treating the observed data as counts, the SPIM method treats each detection as a Bernoulli vector of length equal to the number of traps and a single indicator for which trap made the detection. Augustine et al. (2018) sample the latent capture history by combining the detection vectors into traditional capture history matrices. As a result, SPIM can incorporate additional covariates that provide information on which detections come from which animals (Augustine et al., 2019). In the case when detections are known to be from the same animal (a "must-link" constraint) or known to be from different animals (a "cannot-link" constraint), SPIM uses this information as additional constraints within the MCMC sampler (Augustine et al., 2018). Although SPIM and SC sample the latent animal identities differently within the MCMC, once sampled, they both are equivalent to conventional SCR given the sampled identities.

In ASCR, it is rare that animal identity is known. The conventional model is used to estimate cue density (CD), and then given an independent estimate of cue rate, animal density can be inferred (Stevenson et al., 2015). When individual identity is available, Dawson and Efford (2009) developed a model using the first detected cue by each individual to estimate animal density. More recently, Stevenson et al. (2021) modeled all the detected cues of each individual to estimate animal density when individuals call at fixed locations (ID-ASCR). The time of arrival (TOA) of the vocalization to each microphone provides precise information about where each cue originates. Stevenson et al. (2021) used this spatial information to manually allocate cues to individuals in order to estimate animal density for the Cape Peninsula moss frog.

We derive a general formulation for SCR models with any degree of latent identities, including SCR and ID-ASCR as special cases. This is done by formulating SCR as a marked Poisson process (MPP), in which detection times arise from a counting process and features of detections, such as ID, detection location, and other individual-level features, are treated as marks. Once we have described the MPP framework, we then demonstrate how it can be applied to latent ID SCR (LID-SCR) problems as a mixture model. We then use our framework to estimate density in our motivating examples, the camera trap study of fisher and the acoustic study of frogs. These examples are validated by a simulation study.

2 SPATIAL CAPTURE-RECAPTURE

2.1 Survey methods

We define a detector as a device, such as a camera or a microphone, that records the presence of an animal and the time of the detection. The survey has J detectors set up at locations $\boldsymbol{X} = \{\boldsymbol{x}_1, \ldots, \boldsymbol{x}_J\}$ in a survey region with area A. The detectors are active for a time period T. Within the region, there are N animals at risk of detection, of which the study detects K, and we wish to infer N. In this section, we focus on a survey using cameras as detectors.

The key notation is illustrated in Figure 1. This figure shows $J = 4$ detectors A to D, and activity centers for 2 animals $k = 1, 2$. There was a total of $n_{..} = 9$ detections. Animal 1 was detected twice by detector A ($n_{11} = 2$) and 3 times by C ($n_{13} = 3$); animal 2 was detected once by B ($n_{22} = 1$), once by C ($n_{23} = 1$), and twice by D ($n_{24} = 2$). The resulting animal indicators δ_i ($i = 1, \ldots, 9$) identify which animal detection i corresponds to, the detector indicators $\boldsymbol{\omega} = \{\omega_1, \ldots, \omega_9\}$ specify which detector made each detection, and the detection times are $\boldsymbol{t} = \{t_1, \ldots, t_9\}$. The animal indicator $\boldsymbol{\delta} = \{\delta_1, \ldots, \delta_9\}$ is only observed when animals are individually identifiable on detection; otherwise it is latent.

At the end of the study, detector j has made n_{kj} detections of animal k. When ID is known, a conventional capture history for animal k is $\boldsymbol{n}_k = \{n_{k1}, \ldots, n_{kJ}\}$. When identity is unknown, we observe $n_{.j} = \sum_{k=1}^{N} n_{kj}$ detections at detector j, where N is the number of animals at risk of detection. We assume that N is constant throughout the survey period (ie, we have a closed population). Across all detectors in the study, a total of $n_{..} = \sum_{j=1}^{J} n_{.j}$ detections are made. We assume that detections of each animal follow a Poisson process.

When the rate of the Poisson process is the same for all animals $k = 1, \ldots, N$, the detection times, $\boldsymbol{t}$, are uninformative about N, whether the Poisson process is homogeneous or nonhomogeneous, and are therefore not required to obtain inference about N (Borchers et al., 2014; Schofield et al., 2018). We will focus on the homogeneous Poisson process (HPP), but keep detection times in our description of the model to differentiate the Poisson process from the Poisson distribution. The ideas presented here generalize to the nonhomogeneous case.

2.2 Marked Poisson process

We assume animal k ($k = 1, \ldots, N$) has an activity center, $\boldsymbol{s}_k$, that remains fixed through the survey period but is unobserved. The probability density function (PDF) of $\boldsymbol{s}_k$ is $f(\boldsymbol{s}_k) = D(\boldsymbol{s}_k)/\int_A D(\boldsymbol{s})d\boldsymbol{s}$, where $D(\boldsymbol{s})$ is the intensity of the point process that governs activity centers, at $\boldsymbol{s}$ (Borchers and Efford, 2008). Activity centers are assumed to be independently and identically distributed in the survey region. For notational simplicity, we denote both probability mass functions and PDFs as $f(\cdot)$.

Animal k, with activity center $\boldsymbol{s}_k$, is observed at detector j ($j = 1, \ldots, J$) according to a spatially thinned HPP with rate $h(t, \boldsymbol{x}_j, \boldsymbol{s}_k) = \lambda g(\boldsymbol{x}_j, \boldsymbol{s}_k)$ per unit time at time t (Borchers et al., 2014). Here $g(\boldsymbol{x}_j, \boldsymbol{s}_k)$ is a detection function that is a decreasing function of distance, $d(\boldsymbol{x}_j, \boldsymbol{s}_k) = ||\boldsymbol{x}_j - \boldsymbol{s}_k||$ between detector j and activity center k, and λ is the rate of detections at detector j, for an animal with $d(\boldsymbol{x}_j, \boldsymbol{s}_k) = 0$. A popular detection function is the half-normal, $g(\boldsymbol{x}_j, \boldsymbol{s}_k) = \exp\{-d(\boldsymbol{x}_j, \boldsymbol{s}_k)^2/(2\sigma^2)\}$, where $\sigma \in \mathcal{R}^+$ is referred to as the scale parameter. This detection function arises as the limiting distribution of an Ornstein-Uhlenbeck process for animal movement (McClintock et al., 2022).

With the above HPP, $n_{kj} \sim \text{Poisson}\{H(\boldsymbol{x}_j, \boldsymbol{s}_k)\}$, where $H(\boldsymbol{x}_j, \boldsymbol{s}_k) = \int_0^T h(t, \boldsymbol{x}_j, \boldsymbol{s}_k)dt$ ($k = 1, \ldots, N$; $j = 1, \ldots, J$). Further, if activity centers are located independently, any sum of the n_{kj} is also a Poisson random variable with expected value

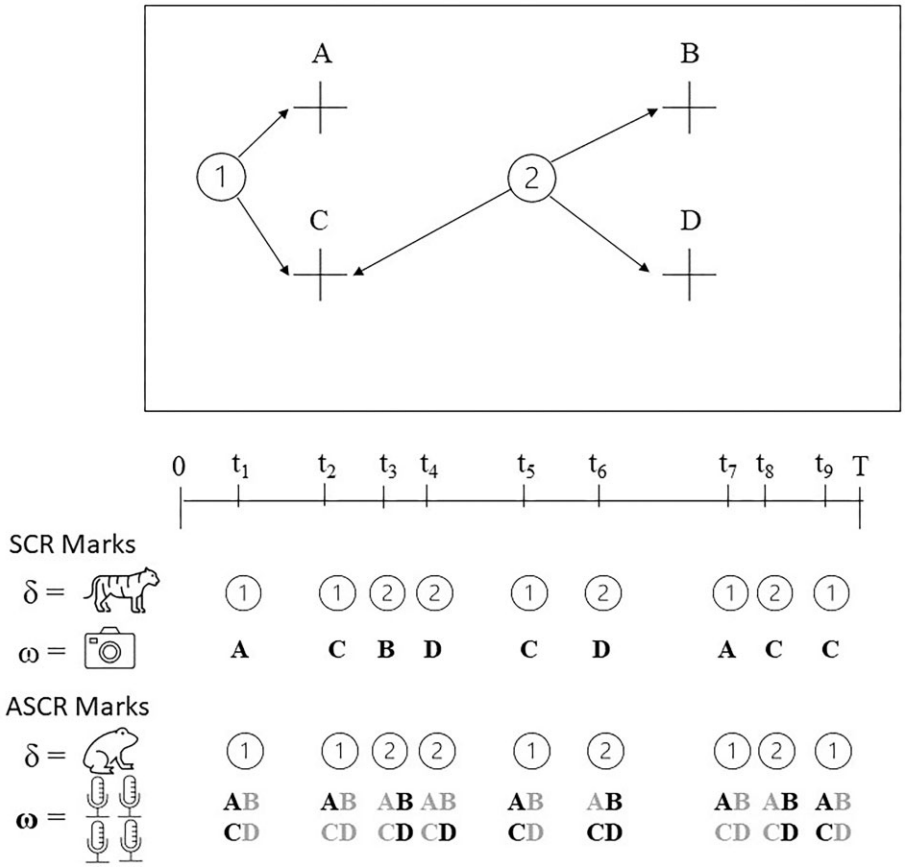

FIGURE 1 Illustrative example of the detection generating process in space and time. Two animal activity centers are shown by numbers in circles. Detectors are crosses named "A", "B", "C", and "D". Arrows show which detectors each animal was detected by. For SCR, each detection is a single animal at a single detector; detection 1 is defined as $\{t_1, \delta_1 = 1, \omega_1 = A\}$. For ASCR, each detection is a single vocalization that can be heard at multiple detectors, while the time the cue is produced, t_1, is latent $\{\delta_1 = 1, \boldsymbol{\omega}_1 = (1, 0, 1, 0)\}$. Abbreviations: ASCR, acoustic SCR; SCR, spatial capture-recapture.

TABLE 1 Notation for the counting process.

Count	Latent	Rate	Expected count
Animal k at detector j (n_{kj})	T	$h(t, \boldsymbol{x}_j, \boldsymbol{s}_k) = \lambda g(\boldsymbol{x}_j, \boldsymbol{s}_k)$	$H(\boldsymbol{x}_j, \boldsymbol{s}_k)$
All animals at detector j $(n_{\cdot j})$	F	$h(t, \boldsymbol{x}_j, \boldsymbol{S}) = \sum_{k=1}^{N} h(t, \boldsymbol{x}_j, \boldsymbol{s}_k)$	$H(\boldsymbol{x}_j, \boldsymbol{S})$
Animal k across all detectors $(n_{k\cdot})$	T	$h(t, \boldsymbol{X}, \boldsymbol{s}_k) = \sum_{j=1}^{J} h(t, \boldsymbol{x}_j, \boldsymbol{s}_k)$	$H(\boldsymbol{X}, \boldsymbol{s}_k)$
All detections $(n_{\cdot\cdot})$	F	$h(t, \boldsymbol{X}, \boldsymbol{S}) = \sum_{k=1}^{N} h(t, \boldsymbol{X}, \boldsymbol{S})$	$H(\boldsymbol{X}, \boldsymbol{S})$

Latent describes detection events that do not depend on identity (Latent = F) and events that depend on identity (Latent = T); λ is the rate under perfect detection, and $g(\boldsymbol{x}_j, \boldsymbol{s}_k)$is the detection function for a detector at $\boldsymbol{x}_j$ and an animal with an activity center at $\boldsymbol{s}_k$. In all cases, the expected count of events in the study period is defined as $H(\cdot) = \int_{t=0}^{T} h(t, \cdot)dt$.

equal to the sum of the relevant expected counts, $H(\boldsymbol{x}_j, \boldsymbol{s}_k)$. See Table 1 for the definitions of the various sums and their associated rates. Note that SC models treat $n_{\cdot j}$, the total number of detections at each detector, as the unit of observation. Instead, we consider the counting process for all $n_{\cdot\cdot}$ detections.

We now describe SCR as a MPP. The $n_{\cdot\cdot}$ detections across all detectors at times $\boldsymbol{t} = (t_1, \ldots, t_{n_{\cdot\cdot}})$ arise from an HPP with rate $h(t_i, \boldsymbol{X}, \boldsymbol{S})$ for $i = 1, \ldots, n_{\cdot\cdot}$, given N animal activity centers located at $\boldsymbol{S} = \{\boldsymbol{s}_1, \ldots, \boldsymbol{s}_N\}$. Note that under an HPP, the rate is not a function of time, $h(t_i, \boldsymbol{X}, \boldsymbol{S}) \equiv h(\boldsymbol{X}, \boldsymbol{S})$. Each event is associated with a mark, defined at minimum as the animal identity, δ_i, and where it was detected, ω_i. It follows from the Poisson process and Table 1 that the animal identity mark, conditional on being detected from one of N animals located at $\boldsymbol{S}$, is categorically distributed,

$$f(\delta_i = k | t_i, \boldsymbol{S}, N) = \frac{h(t_i, \boldsymbol{X}, \boldsymbol{s}_k)}{h(t_i, \boldsymbol{X}, \boldsymbol{S})}, \tag{1}$$

for $\delta_i \in \{1, \ldots, N\}$. Similarly, given $\delta_i = k$, the detector mark is also categorically distributed,

$$f(\omega_i = j | t_i, \delta_i = k, \boldsymbol{S}, N) = \frac{h(t_i, \boldsymbol{x}_j, \boldsymbol{s}_k)}{h(t_i, \boldsymbol{X}, \boldsymbol{s}_k)}, \tag{2}$$

for $\omega_i \in \{1, \ldots, J\}$.

Given the $n_{\cdot\cdot}$ detections at times $\boldsymbol{t}$, the joint mark distribution for the specific animals detected, $\boldsymbol{\delta} = \{\delta_1, \ldots, \delta_{n_{\cdot\cdot}}\}$, at detectors

$\boldsymbol{\omega} = \{\omega_i, \ldots, \omega_{n..}\}$, is

$$f(\boldsymbol{\delta}, \boldsymbol{\omega}|n.., \boldsymbol{t}, \boldsymbol{S}, N) = \prod_{i=1}^{n..} f(\delta_i, \omega_i|t_i, \boldsymbol{S}, N) = \prod_{i=1}^{n..} \frac{h(t_i, \boldsymbol{x}_{\omega_i}, \boldsymbol{s}_{\delta_i})}{h(t_i, \boldsymbol{X}, \boldsymbol{S})}. \quad (3)$$

Overall, the observed data $n..$, $\boldsymbol{t}$, $\boldsymbol{\delta}$, and $\boldsymbol{\omega}$ arise from a MPP with marks $\{\boldsymbol{\delta}, \boldsymbol{\omega}\}$, as illustrated in Figure 1, with joint distribution

$$f(n.., \boldsymbol{t}, \boldsymbol{\delta}, \boldsymbol{\omega}|\boldsymbol{S}, N) = f(n..|\boldsymbol{t}, \boldsymbol{S}, N) f(\boldsymbol{\delta}, \boldsymbol{\omega}|n.., \boldsymbol{t}, \boldsymbol{S}, N) = e^{-H(\boldsymbol{X},\boldsymbol{S})} \prod_{i=1}^{n..} h(t_i, \boldsymbol{X}, \boldsymbol{S}) \prod_{i=1}^{n..} \frac{h(t_i, \boldsymbol{x}_{\omega_i}, \boldsymbol{s}_{\delta_i})}{h(t_i, \boldsymbol{X}, \boldsymbol{S})} \quad (4)$$

$$= e^{-H(\boldsymbol{X},\boldsymbol{S})} \prod_{i=1}^{n..} h(t_i, \boldsymbol{x}_{\omega_i}, \boldsymbol{s}_{\delta_i}). \quad (5)$$

Equation 5 shows that the MPP is equivalent to the continuous-time SCR model in Equation 2 of Borchers et al. (2014). However, the MPP provides a new way of thinking about the detection process in continuous time. Generally, SCR approaches model detections conditionally on animal and detector identity, but here we show how these quantities can be modeled jointly. This allows us to model SCR as a counting process that does not depend on animal identities, and a mark distribution that does, providing an explicit link to continuous time capture-recapture as presented in Schofield et al. (2018).

As we are assuming an HPP, the rest of this manuscript will consider likelihoods in which detection times are marginalized out, modeling the count of detections $(n..|\boldsymbol{S}, N) \sim \text{Poisson}\{H(\boldsymbol{X}, \boldsymbol{S})\}$ and the associated mark distribution $f(\boldsymbol{\delta}, \boldsymbol{\omega}|n.., \boldsymbol{S}, N)$ that does not depend on when the events occur.

3 ACOUSTIC SCR

In ASCR, an acoustic cue (a vocalization) is produced at some activity center $\boldsymbol{s}_k$ and the cue propagates through space, while the probability of detecting it decreases with distance. For ID-ASCR described by Stevenson et al. (2021), we assume that animals produce cues according to an HPP with rate λ per unit time and that the animal remains at a fixed activity center for the duration of the survey. Cue i is produced by animal $k = \delta_i$, at time t_i, and is detected by detector j (event $\omega_{ij} = 1$), with probability decreasing with distance, $d(\boldsymbol{x}_j, \boldsymbol{s}_k)$. A common detection function in ASCR is the hazard half-normal, $g(\boldsymbol{x}_j, \boldsymbol{s}_k) = 1 - \exp[-g_0 \exp\{-d(\boldsymbol{x}_j, \boldsymbol{s}_k)^2/(2\sigma^2)\}]$ where $g_0, \sigma \in \mathcal{R}^+$. In ASCR, a detection must be accurately assigned to the cue that produced it.

Under our new MPP formulation, the detection mark is a Bernoulli vector $\boldsymbol{\omega}_i$, indicating which detectors detected cue i. The probability that cue i, produced by animal k, is detected at least once is $g_.(\boldsymbol{X}, \boldsymbol{s}_k) = \mathbb{P}(c_i > 0|\boldsymbol{s}_k) = 1 - \prod_{j=1}^{J}\{1 - g(\boldsymbol{x}_j, \boldsymbol{s}_k)\}$, for $c_i = \sum_{j=1}^{J} \omega_{ij}$. Then,

$$f(\boldsymbol{\omega}_i|\delta_i, \boldsymbol{S}, N) = \frac{\prod_{j=1}^{J} g(\boldsymbol{x}_j, \boldsymbol{s}_{\delta_i})^{\omega_{ij}}\{1 - g(\boldsymbol{x}_j, \boldsymbol{s}_{\delta_i})\}^{1-\omega_{ij}}}{g_.(\boldsymbol{X}, \boldsymbol{s}_{\delta_i})}. \quad (6)$$

Note that conditioning on an animal having produced the detected cue, δ_i, implies that the cue was detected, $c_i > 0$.

Animal k $(k = 1, \ldots, N)$ produces detected cues according to a thinned HPP with rate $h(\boldsymbol{X}, \boldsymbol{s}_k) = \lambda g_.(\boldsymbol{X}, \boldsymbol{s}_k)$ per unit time. The rate of detected cues across all detectors is $h(\boldsymbol{X}, \boldsymbol{S}) = \sum_{k=1}^{N} h(\boldsymbol{X}, \boldsymbol{s}_k)$. The expected number of detections in the survey is then $H(\boldsymbol{X}, \boldsymbol{S}) = T \times h(\boldsymbol{X}, \boldsymbol{S})$. The animal ID mark, δ_i, is categorically distributed as in Equation 1, $f(\delta_i = k|t_i, \boldsymbol{S}, N) \propto h(\boldsymbol{X}, \boldsymbol{s}_k)$. The $n.. \times J$ matrix of capture histories, $\boldsymbol{\omega}_i$, is denoted by Ω. Figure 1 illustrates the process of detections on 4 detectors through time, showing how the vector detector mark, $\boldsymbol{\omega}_i$, differentiates ASCR from SCR.

In ASCR, we detect cue i, on detector j, at time y_{ij}, a short time after the unknown time of cue production t_i. Given the speed of sound v, we assume the TOA of the cue at the detector is observed with Gaussian error, $(y_{ij}|\omega_{ij} = 1, t_i) \sim \mathbb{N}(t_i + d(\boldsymbol{x}_j, \boldsymbol{s}_k)/v, \sigma_t)$. By assuming the cues occur according to an HPP, marginalizing $f(\boldsymbol{y}_i, t_i|\cdot)$ over the cue production time, Borchers et al. (2015) obtained the following expression for the PDF of times of detected calls, $\boldsymbol{y}_i$, given δ_i and $\boldsymbol{\omega}_i$,

$$f(\boldsymbol{y}_i|\boldsymbol{\omega}_i, \delta_i, \boldsymbol{S}, N) = \begin{cases} (T\sqrt{c_i})^{-1}(2\pi\sigma_t^2)^{(1-c_i)/2}\exp\{-(2\sigma_t^2)^{-1}\sum_{j=1}^{J}\omega_{ij}(\gamma_{ij} - \bar{\gamma}_i)^2\} & c_i > 1 \\ 1 & c_i = 1. \end{cases} \quad (7)$$

Here, $\gamma_{ij} = y_{ij} + d_{\delta_i j}/v$ and $\bar{\gamma}_i = \sum_{j=1}^{J} c_i^{-1}\omega_{ij}\gamma_{ij}$.

We now have the distribution for marks $\{\boldsymbol{\delta}, \Omega, \boldsymbol{Y}\}$, where $\boldsymbol{Y} = \{\boldsymbol{y}_i, \ldots, \boldsymbol{y}_{n..}\}$,

$$f(\boldsymbol{\delta}, \Omega, \boldsymbol{Y}|n.., \boldsymbol{S}, N) = \prod_{i=1}^{n..} f(\delta_i|\boldsymbol{S}, N) f(\boldsymbol{\omega}_i|\delta_i, \boldsymbol{S}, N) \times f(\boldsymbol{y}_i|\boldsymbol{\omega}_i, \delta_i, \boldsymbol{S}, N). \quad (8)$$

When we use Equation 8 for the mark distribution of the MPP, the likelihood is proportional to the ID-ASCR likelihood of Stevenson et al. (2021).

4 LATENT ID SCR

As shown above, we can formulate conventional SCR such that animal identity, δ_i, is treated as a mark arising from a categorical distribution. The other detected marks, $\boldsymbol{m}_i$, are modeled conditionally on the animal's identity, which is defined by its activity center. As a result, when δ_i is latent, the observed marks $\boldsymbol{m}_i$ (SCR: $\boldsymbol{m}_i = \{\omega_i\}$ as in Equation 2, ASCR: $\boldsymbol{m}_i = \{\boldsymbol{\omega}_i, \boldsymbol{y}_i\}$ as in Equation 8) can be modeled as if they arise from a mixture of N mark distributions conditional on the activity centers $\boldsymbol{S}$, with mixture probabilities $\pi_k = f(\delta_i = k|\boldsymbol{S}, N)$. Thus $f(\boldsymbol{m}_i|\boldsymbol{S}, N) = \sum_{k=1}^{N} \pi_k f(\boldsymbol{m}_i|\delta_i = k, \boldsymbol{s}_k)$. The

mixture weights, $\boldsymbol{\pi} = \{\pi_1, \ldots, \pi_N\}$, have a parametric form defined by the Poisson process in Equation 1 and depend only on the distance of each animal to all detectors.

In standard mixture model notation, we write the joint distribution for all $n_{..}$ observed marks, $\boldsymbol{M} = \{\boldsymbol{m}_1, \ldots, \boldsymbol{m}_{n_{..}}\}$, marginalizing over all the mixture components, $\boldsymbol{\delta}$, as

$$f(n_{..}, \boldsymbol{M}|\boldsymbol{S}, N) = f(n_{..}|\boldsymbol{S}, N) \prod_{i=1}^{n_{..}} \sum_{k=1}^{N} \pi_k f(\boldsymbol{m}_i|\delta_i = k, \boldsymbol{s}_k). \tag{9}$$

In a Bayesian framework, the posterior distribution, including all model parameters, $\boldsymbol{\theta}$, to be estimated in Equation 9 is,

$$f(\boldsymbol{\theta}, \boldsymbol{S}, N|n_{..}, \boldsymbol{M}) \propto f(n_{..}, \boldsymbol{M}|\boldsymbol{S}, N) \times f(\boldsymbol{S}|N) f(N) f(\boldsymbol{\theta}). \tag{10}$$

Under SCR, $\boldsymbol{\theta} = \{\lambda, \sigma, \boldsymbol{\theta}_D\}$, and ASCR $\boldsymbol{\theta} = \{\lambda, \sigma, g_0, \sigma_t, \boldsymbol{\theta}_D\}$. Here, $\boldsymbol{\theta}_D$ represents any parameters relating to the density process, $D(\boldsymbol{s})$. The SC model in Chandler and Royle (2013) is a special case of Equation 10.

4.1 Estimation

When we consider the model as a standard finite mixture model with an uncertain number of clusters (animals), there is a wide variety of fitting methods to choose from. A Bayesian approach using MCMC is attractive for a model-based solution to the unknown number of clusters problem. For this, we use a fixed parameter space and apply data augmentation, a common approach in the SCR literature for estimating unobserved animals for both known ID and latent ID scenarios (Tanner and Wong, 1987; Royle and Dorazio, 2012; Chandler and Royle, 2013; Augustine et al., 2018). For classical marginal likelihood methods, both $\boldsymbol{S}$ and N must be integrated out of the likelihood. However, this poses a computational challenge as the integration of $\boldsymbol{S}$ has dimension $N \times 2$.

In the context of SCR, data augmentation assigns a superpopulation of L individuals, such that $N << L$ and uses indicators z_k to reference whether animal $k = 1, \ldots, L$ is available to be detected, $z_k = 1$, or not, $z_k = 0$, with $z_k \sim \text{Bernoulli}(\psi)$, for hyperparameter ψ (Royle and Dorazio, 2012). We define the population size as the number of animals available for detection, $N = \sum_{k=1}^{L} z_k$. This method fixes the dimension of the parameter space, which allows the use of standard MCMC sampling algorithms. Setting $\psi \sim \text{Beta}(1, 1)$ is equivalent to using a prior distribution of $N \sim \text{Discrete-Uniform}(0, L)$, and is the preferred approach in the existing literature (Chandler and Royle, 2013; Sollmann et al., 2013; Augustine et al., 2018; Jiménez et al., 2021). Link (2013) recommends a scale prior such that $f(N) \propto \frac{1}{N}$. However, for LID-SCR, we must often differentiate between a small N and large σ, or a large N and small σ, and an inverse prior on N can have a heavy influence. Biologists often have strong prior information about the animal's home range, so it makes more sense to put an informative prior on σ while assigning a flat prior on N. This situation was exemplified in the parula analysis from Chandler and Royle (2013) when, using a flat prior on N, the posterior mode and 95% credible interval were $\widehat{N} = 4\,(3, 432)$ when the home range scale parameter was $\sigma \sim \text{U}(0, \infty)$, but $\widehat{N} = 36\,(18, 157)$ when the informative prior, $\text{Gamma}(13, 10)$, was used.

To simplify the MCMC algorithm, we use data augmentation for both $\boldsymbol{\delta}$ and $\boldsymbol{z}$ to sample from the complete-data likelihood (Tanner and Wong, 1987). The posterior distribution is given by

$$f(\boldsymbol{\theta}, \boldsymbol{\delta}, \boldsymbol{S}, \boldsymbol{z}|n_{..}, \boldsymbol{M}) \propto f(n_{..}|\boldsymbol{S}, \boldsymbol{z}) f(\boldsymbol{\delta}, \boldsymbol{M}|\boldsymbol{S}, \boldsymbol{z}) f(\boldsymbol{S}) f(\boldsymbol{z}) f(\boldsymbol{\theta}), \tag{11}$$

where $f(\boldsymbol{\delta}, \boldsymbol{M}|\boldsymbol{S}, \boldsymbol{z})$ is given by Equations 3 and 8 for SCR and ASCR, respectively. By introducing $\boldsymbol{z}$, we no longer condition on N animals, as this information is contained in $\boldsymbol{z}$ with fixed length L. However, we now define a new rate, $h(\boldsymbol{x}_j, \boldsymbol{s}_k, z_k) = z_k h(\boldsymbol{x}_j, \boldsymbol{s}_k)$. Only animals at risk of detection contribute to the counting process, $n_{..}|\boldsymbol{S}, \boldsymbol{z} \sim \text{Poisson}(H(\boldsymbol{X}, \boldsymbol{S}, \boldsymbol{z}))$. Additionally, following Equation 11, we sample the latent animal identities $\boldsymbol{\delta}$.

From Equation 11, the full-conditional distribution for δ_i is,

$$f(\delta_i = k|\cdot) \propto z_k f(\delta_i = k|\boldsymbol{S}, \boldsymbol{z}) f(\boldsymbol{m}_i|\delta_i = k, \boldsymbol{s}_k, z_k), \tag{12}$$

for $k = 1, \ldots, L$. The mark distribution, $f(\boldsymbol{m}_i|\delta_i = k, \boldsymbol{s}_k, z_k)$, is defined for SCR in Equation 2 and ASCR in Equation 8, and $f(\delta_i = k|\boldsymbol{S}, \boldsymbol{z})$ is the mixture weight defined by Equation 1.

As with mixture models in general, this model suffers from nonidentifiability in the animal location for each index k, also referred to as "label switching" (Jasra et al., 2005). An animal k may be unobserved ($n_{k\cdot} = 0$ and $z_k = 1$), not available for detection ($z_k = 0$), or allocated to detections ($n_{k\cdot} > 0$ and $z_k = 1$). Each allocation of detections is associated with a different posterior mode for $\boldsymbol{s}_k$. As a result, the distribution of each activity center, $\boldsymbol{s}_k$, is multimodal resulting in poor mixing when using adaptive procedures. A solution for this is to use a fixed-scale random walk sampler or to use a proposal distribution that leads to both local updates and jumps to other modes to improve mixing. We know that the full-conditional of $\boldsymbol{s}_k$, when $z_k = 0$, is $f(\boldsymbol{s}_k)$, as given at the start of Section 2.2. For this reason, when animals are uniformly distributed in space, we use a Metropolis-Hastings sampler with proposals from a mixture distribution,

$$\boldsymbol{s}_k^*|\boldsymbol{s}_k \sim a_0 \mathcal{N}(\boldsymbol{s}_k, b_0) + (1 - a_0)\mathcal{U}(A), \tag{13}$$

where $\boldsymbol{s}_k^*$ is the proposed new value for $\boldsymbol{s}_k$. The user sets the mixture proportion $a_0 \in [0, 1]$ and the scale $b_0 \in \mathcal{R}^+$ as tuning parameters. $\mathcal{U}(A)$ represents a uniform distribution over the survey region with area A. Guidance for choosing a_0 is given in Web Appendix A.

We implemented an MCMC sampler using the software Nimble (de Valpine et al., 2017; 2020) within R (R Core Team, 2019). The default sampling algorithm used by Nimble for continuous-valued parameters is adaptive Metropolis-Hastings random walk sampling (Haario et al., 2001). Due to the highly correlated nature of σ with both λ and ψ, we use Nimble's standard fixed width slice sampler for σ to improve mixing (Neal, 2003). The remaining parameters of the model can be sampled using standard SCR MCMC methods presented for Nimble by Turek et al. (2021). We note that when the mixture weights are only dependent on the animal activity centers, $\boldsymbol{S}$, it is not necessary to allocate detections and we can sample from the posterior described in Equation 10. This is commonly used for SC

models including when the population is partially identifiable (Chandler and Royle, 2013; Sollmann et al., 2013; Whittington et al., 2018). All the details of the MCMC algorithm are provided in Web Appendix B along with code.

5 APPLICATIONS

5.1 Spatial capture-recapture

5.1.1 Fisher camera trap study

In Alberta's UNESCO Beaver Hill Biosphere Reserve, Canada, 64 baited camera traps were set from January 1 to April 30, 2016 to monitor fisher (*Pekania pennanti*) using baited stations, replaced monthly. Motion-sensitive camera traps were deployed in a systematic design on a 4 × 4 km grid cell (Web Figure 1); see Burgar et al. (2018) for a full description of the survey methods. Stewart et al. (2017) carried out a genetic hair snag study (January-April) paired with the camera trap survey. An earlier live-trapping study was also conducted (November 2015-January 2016), where a total of 14 collars were attached to 5 male and 9 female individuals, as described in Stewart et al. (2019). Burgar et al. (2018) used the genetic data from the concurrent hair snag study (24 unique individuals; 9 male, 14 female) to implement known ID SCR with each month as a discrete occasion. They estimated animal density to be 2.96 (2.18, 4.72) individuals per 100 km^2, which is similar to published estimates on the species (eg, Linden et al., 2017). Genetic data were also collected in the live-trapping study, allowing individuals to be matched between the 2 surveys (Web Appendix A, Table 1).

In March and April, it is thought that female fisher change their behavior in preparation for birth and mating. Following Burgar et al. (2018), to remove the potential for confounding with behavioral effects, we limited our analysis of the camera trap data to the end of March 4. The combined known ID surveys over this period detected a total of 24 individuals (8 males and 15 females), with 11 recaptures of the live-trapped individuals by hair snag. We use these data to evaluate the accuracy of our latent ID model using the camera trap data.

Each photograph was marked with sex (male/female) and collar (present/absent) when the quality of the image permitted. A total of 207 detections were made over the 64 days. Sex was observable in 32% of the images, 42 female and 24 male. Additionally, 40% gave collar information, 52 as uncollared, and 32 as collared. The collars were not uniquely distinguishable so that when they were identified as present, we only learned that the animal had been previously physically trapped and collared, similar to a batch marking survey. For animal k, we define the additional characteristics: sex x_{k2} (male $x_{k2} = 0$ or female $x_{k2} = 1$), and collar x_{k3} (uncollared $x_{k3} = 0$ or collared $x_{k3} = 1$). The animal's sex is distributed as $x_{k2} \sim \text{Bernoulli}(\gamma)$, where γ is the population proportion of females. The collars were assigned to animals $k = 1, \ldots, 14$ in our fitting algorithm, $(x_{k3} = 1)$, while animals $k = 15, \ldots, L$ were uncollared $(x_{k3} = 0)$. For the collared individuals, we assign sex, $x_{k2} = 0$ for $k = 1, \ldots, 5$ and $x_{k2} = 1$ for $k = 6, \ldots, 14$. The observed marks for detection i in our model are therefore the camera trap $m_{i1} = \omega_i$, sex m_{i2}, and collar m_{i3}. Marks are assumed observed without error. The joint mark distribution for a single detection, i, conditional on the animal characteristics $\boldsymbol{x}$ and activity centers $\boldsymbol{S}$, is

$$f(\boldsymbol{m}_i|\delta_i, \boldsymbol{x}, \boldsymbol{S}, N) = f(\omega_i|\delta_i, \boldsymbol{S}, N) I(m_{i2} = x_{\delta_i 2}) \times I(m_{i3} = x_{\delta_i 3}), \quad (14)$$

where $I(\cdot)$ is an indicator function indicating that the detection must match the animal characteristic. When the additional marks are missing, we marginalize over the mark. For matching the collared detections to animals, we adjust the animal collar status of the 14 individuals based on the time when animals were first collared. For example, at the beginning of January, only 12 animals were collared, leaving the potential for an uncollared detection in early January to be allocated to 1 of the 2 individuals collared by mid-January.

We consider 2 different inferential approaches for the fisher camera trap data. As previously noted, because of the parametric form of the mixture weights, we can sample the marginalized model from Equation 9 directly, or we can sample the animal identities. Additionally, we compare results from 4 different models with varying amounts of mark information: (1) just the observed trap mark with marginalized ID (SC), (2) allocating ID (LID) using the full-conditional in Equation 12, (3) adding sex as a mark (LID+Sex), and (4) adding both sex and collar marks (LID+Sex/Collar). Prior distributions on all parameters were uniform with ranges that did not constrain the posterior (see Web Appendix A for details). Inferences drawn from Model 1 are equivalent to those from Algorithm 2 in Chandler and Royle (2013) and for computational purposes, we aggregated the counts at each trap, reducing exactly to the SC model.

Results of the analysis are shown in Figure 2. For each model, 3 chains were run, each for 60 000 iterations after an initial 40 000 burn-in. We visually inspected trace plots to assess the convergence, which was deemed satisfactory. Allocating ID gives nearly equivalent results to the SC model as expected. However, the SC model has improved mixing over N, as it avoids the more complicated allocation step. Both SC and LID densities are right-skewed and lack precision, with mode and 95% credible interval, $\widehat{D} = 2.2$ (1.3, 7.9) individuals per 100 km^2 (from model 2). Note that due to the right-skew posterior distributions of these models, we use the posterior mode as the point estimate.

Web Figure 1 highlights that any activity center equidistant from a camera trap has an equivalent probability of producing the detection. Count correlation between traps helps to inform where activity centers can or cannot be, but the detector mark, ω_i, alone does not contribute much to the estimation of density. Adding sex alone decreased precision and increased the population density estimate $\widehat{D} = 3.3$ (2.1, 15.4). This is likely because sex was not perfectly observed and may highlight problems with the model assumptions such as independence between male and female home ranges. In this case, separating detections by sex may not be very informative.

Using both collar and sex in model 4 resulted in a large improvement to the precision of density, $\widehat{D} = 2.0$ (1.5, 2.9). Importantly, the model 4 posterior mean of σ ($\widehat{\sigma} = 1.9$ (1.6, 2.2)) increased compared to the estimates from the other models and was more similar to that from the genetic SCR study $\widehat{\sigma} = 2.5$ (2, 3.5). Model 4 estimated a posterior mean of $\widehat{K} = 26$ unique individuals detected (11 male and 15 female). Of these, 7 were

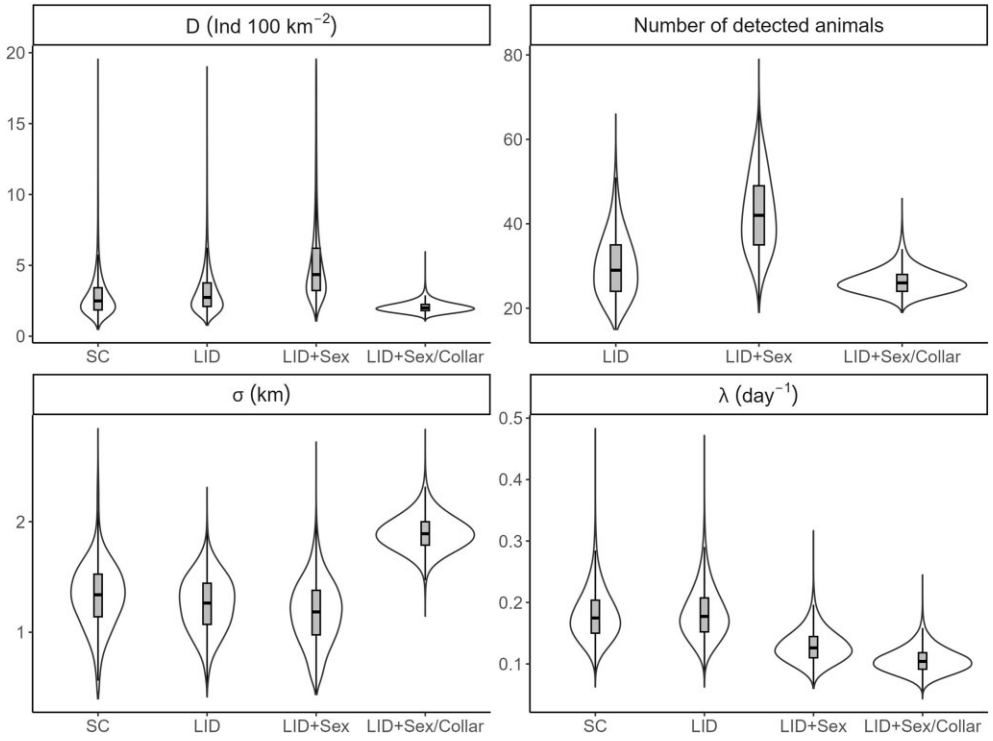

FIGURE 2 Fisher data analysis results for 4 different latent ID SCR models: spatial count (SC), latent ID SCR (LID), LID with Sex as a covariate (LID+Sex), and LID+Sex with the collar information included (LID+Sex/Collar). D is animal density, σ is the scale parameter in the detection function, and λ is the detection intensity at a trap per unit time for an animal at distance 0. We ran the MCMC algorithm using 3 chains for 60 000 iterations after an initial 40 000 burn-in. Posterior plots are shown as violin plots with the interior boxplots showing 50% credible intervals and the median. Abbreviation: MCMC, Markov Chain Monte Carlo.

collared (3 male and 4 female), an exact match to the recaptures in the genetic study of collared individuals for the same months (Web Table 1). The estimate of density is slightly smaller than the 1 from the genetic study by Burgar et al. (2018) ($\widehat{D} = 2.96$ (2.18, 4.72)). See Web Appendix A for a detailed discussion on these differences. The performance of models 2, 3, and 4 is tested further using a simulation study.

5.1.2 *Simulation*

To validate the 3 latent ID models, we investigated through simulation 2 possible scenarios with 3 different models: LID, LID+Sex, and LID+Sex/Collar. The parameter values were based on the results from the fisher study with 2 levels of density and detectability: scenario 1 ($D = 2.44$, $N = 50$, $\sigma = 1.5$, $\lambda = 0.15$) and scenario 2 ($D = 1.95$, $N = 40$, $\sigma = 2.0$, $\lambda = 0.10$). We used the fisher survey design of 64 traps over 64 days with a survey area of 20.5×100 km^2. In both scenarios, we randomly allocated collars to 14 individuals (5 male and 9 female), and we assumed the probability of an animal being female was $\gamma = 0.60$. Detections were randomly selected to be of high enough quality to identify sex and/or collar status with probabilities 0.32 and 0.40, respectively.

For each scenario, 100 datasets were simulated and then analyzed using the 3 models. For each model, a single chain was run for 60 000 iterations with the first 20 000 removed as burn-in. Three chains were used for a portion of simulations to check for consistent convergence (see Web Appendix B for details). The results in Figure 3 show relative bias for each simulated dataset and method where relative percentage bias is $100 \times \frac{\widehat{\theta}-\theta}{\theta}$, for any parameter θ and point estimate $\widehat{\theta}$.

The distribution of the sampled means and medians were both highly right-skewed for density, $\widehat{D} = \widehat{N}/A$, and they did not act as an unbiased point estimate except when both sex and collar information was used. Similarly to other studies, we found the posterior marginal mode to be nearly unbiased and as we adopt uniform priors, we expect that this point estimator is likely to be relevant when one compares inferences with frequentist analyses. However, the models generally performed poorly when relying only on the detector mark. Including both the partially observed sex and collar marks increased the precision and decreased bias in all scenarios. Increasing the amount of overlap between animal home ranges decreased the performance of these models. This is controlled by both σ and D. For scenario 2, increasing σ and reducing D resulted in similar performance to Scenario 1. The LID+Sex/Collar model estimates were nearly unbiased for all parameters and were the most reliable. Our simulation study results highlight the potential for LID-SCR when additional information is available, even if it is only partially observed.

5.2 Acoustic SCR

5.2.1 *Cape peninsula moss frog acoustic study*

We use an acoustic survey of Cape Peninsula moss frog (*Arthroleptella lightfooti*) on Steenberg Plateau in Table Mountain National Park, South Africa, which has previously been used for estimating CD (Stevenson et al., 2015; Measey et al., 2017),

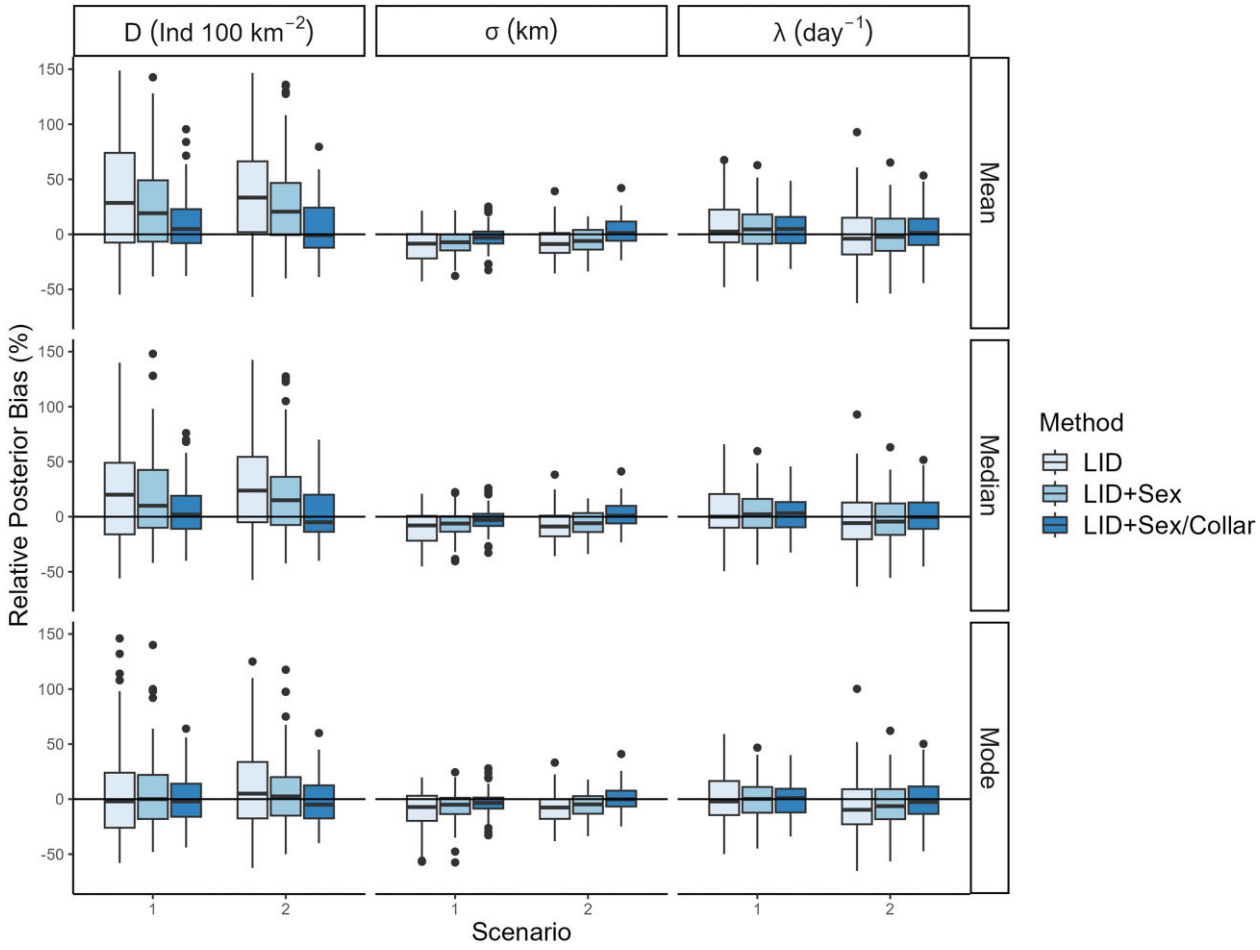

FIGURE 3 Latent identity spatial capture-recapture relative bias for 3 different latent ID SCR models: latent ID SCR (LID), LID with sex as a covariate (LID+Sex), and LID+Sex with the collar information included (LID+Sex/Collar). D is animal density, σ is the scale parameter in the detection function, and λ is the detection intensity at a trap per unit time for an animal at distance 0. We ran the MCMC algorithm for 60 000 iterations with 20 000 burn-in. Relative bias is shown for 3-point estimates of the posterior. The y-axis is cut-off at 150% bias, which removes some outliers of simulation scenarios that did not converge (Web Appendix B). Abbreviation: MCMC, Markov Chain Monte Carlo.

and animal density when ID can be inferred (Stevenson et al., 2021). Moss frogs are very small and cryptic, hiding in shrubs, making traditional count methods unreliable. The males cue to attract a mate and do not move in a calling period.

A 6-channel recorder with a single clock was set up roughly in a circle with microphones spaced approximately 5 m apart (Web Figure 1; full details in Measey et al. (2017)). This enables accurate times of detection to be recorded. Two surveys took place 18 days apart. Due to high cue frequency, each survey period was 30 seconds, for a total of 98 and 86 detected cues. In an *ad hoc* analysis, Stevenson et al. (2021) identified 14 and 9 unique individuals, respectively, in the 2 sampling sessions.

The data were analyzed using ASCR in 3 ways: (1) latent ID (LID), (2) known ID (ID), and (3) CD, where cues are assumed to occur from independent cue locations. As per Stevenson et al. (2021), a half-normal hazard detection function and a constant cue rate were assumed. Prior distributions were all uniform with bounds well beyond the sampled parameter space (see Web Appendix B for details). Potential animal locations were buffered by 15 m beyond the traps. The survey sessions, $r = \{1, 2\}$, were assumed to be independent but shared parameters, and $N_r \sim \text{binomial}(\psi, L)$. For LID-ASCR, we used Equation 12 to allocate detections to animals. The R package "ascr" (Stevenson and Borchers, 2018), which gives maximum likelihood estimates of the cue parameters, was used for CD-ASCR. For models 1 and 2, we ran 3 chains for 30 000 iterations after an initial 20 000 burn-in. Trace plots for all parameters were visually checked for convergence.

Animal density is reported as, $\widehat{D} = \frac{\widehat{\psi} \times L}{A}$ individuals per hectare (ind/Ha). For ID-ASCR, we obtained a posterior marginal mode and 95% credible interval of $\widehat{D} = 368$ (250, 539). For LID-ASCR, our model estimated $\widehat{D} = 389$ (253, 577), which agrees well with the known ID method. We estimated a posterior mean of $\widehat{K} = 27$ (22, 33) detected frogs in the 2 surveys combined which agrees with the 23 inferred by the *ad hoc* analysis. To compare with CD-ASCR, we also estimated CD, $\mu = \lambda \times D$ cues per second per Ha. Using ID-ASCR, the posterior marginal mode was $\widehat{\mu} = 111$ (74, 166), while with the LID-ASCR model it was $\widehat{\mu} = 106$ (72, 161), and with CD-ASCR, we found $\widehat{\mu} = 125$ (104, 145), based on maximum likelihood estimation and 95% confidence interval. See Figure 4 for results on each parameter.

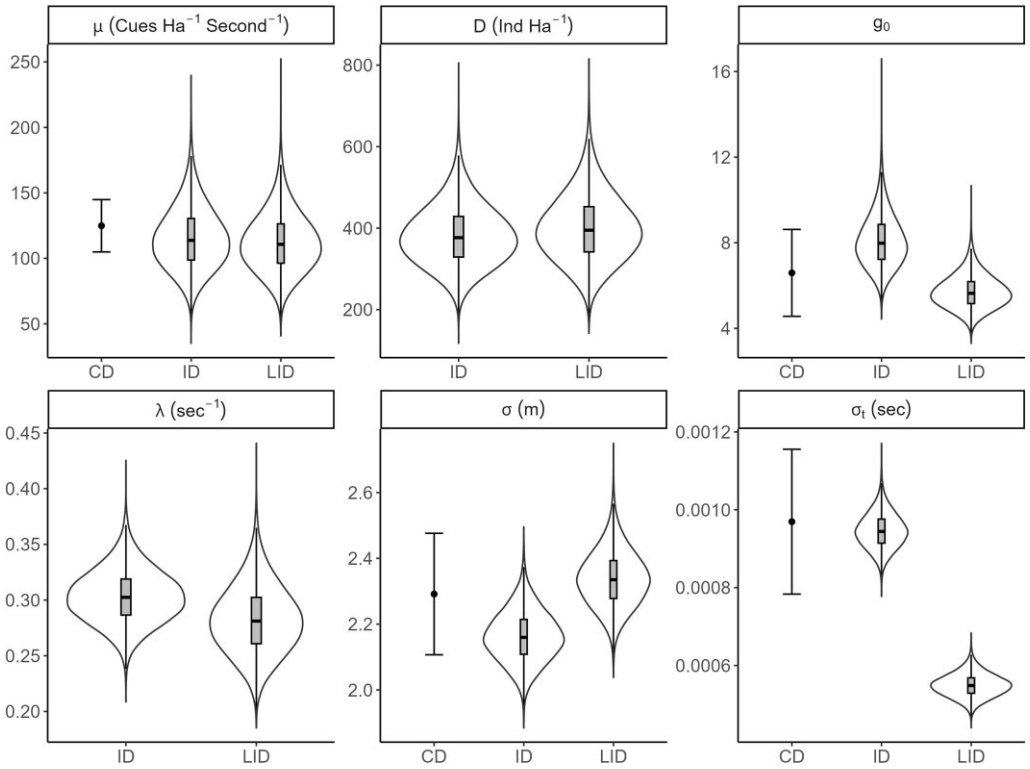

FIGURE 4 Frog data analysis results for 3 different ASCR models: cue density (CD), known ID (ID), and latent ID (LID). Model CD shows the maximum likelihood estimator and 95% confidence intervals; μ is CD, D is animal density, λ is the cue rate, σ is the scale parameter, g_0 is the probability of a cue being recorded at distance 0 from the microphone, and σ_t is the standard error of the time of arrival. Posterior plots are shown as violin plots with the interior boxplots showing 50% of the values and the median. Abbreviation: ASCR, acoustic SCR.

Unlike the camera trap study, each detection in ASCR is associated with multiple traps, which can give accurate information on where the cue originates when there are multiple recaptures of a single cue. With accurate TOA information, we lost very little information about density by not knowing animal ID, accurately recovering the cue rate parameter λ. When cue rate and the detection function are both estimable, animal density can also be estimated (Stevenson et al., 2015). Errors in the data can occur from assigning animal ID via *ad hoc* methods, or when assigning a detection to a single cue. We expect both cases to positively bias σ_t. A simulation study was used to explore the differences in σ_t further.

5.2.2 *Simulation*

To test our latent ID ASCR model, we carried out a simulation study matching the *A. lightfooti* survey design; 6 traps recording for a total of 30 seconds for 2 occasions. The latent ID and known ID models for the real data example differed mainly in their estimate of TOA error, σ_t. We considered the performance of our latent ID model under a simulation study with 3 values of σ_t: (A) $\sigma_t = 0.05$, (B) $\sigma_t = 0.001$, and (C) $\sigma_t = 0.00055$. Scenario A represents an error rate high enough that TOA no longer adds new information to the model about cue location (Web Figure 1). Scenarios B and C were chosen to match the data example. For each scenario, 100 datasets were simulated, and for each model, a single MCMC chain was run for 40 000 iterations, removing the first 20 000 as burn-in. A subset of these simulations were visually inspected for consistent convergence by running multiple chains (See Web Appendix B for details). The population $N = 55$ was held constant between the 2 sessions. Other parameters were $\{D = 408.16, \sigma = 2.3, g_0 = 5.75, \lambda = 0.28\}$.

Results from the simulation study are shown in Figure 5. As expected, for Scenario A, the latent ID model was unable to reliably allocate detections to animals with just 6 microphones, displaying bias in λ and σ. By losing the spatial information for animal ID provided by the additional TOA mark, the simulation results become right-skewed for the mean and median, similar to the camera trap simulations. For scenarios B and C where σ_t is small, all parameters are estimated with little to no bias and improved precision over scenario A. If TOA information is not available, more detectors would be required to reliably perform LID-ASCR density estimation. Our simulation study did not highlight any bias in estimating σ_t.

6 DISCUSSION

Writing SCR as an MPP separates the counting process from the observed marks distribution. This makes the counting process specific and straightforward to generalize to other distributional assumptions, such as a renewal or self-exciting point process (Daley and Vere-Jones, 2003; Rushing, 2023). It also naturally links continuous-time SCR (Borchers et al., 2014), ID-ASCR (Stevenson et al., 2021), and continuous-time non-SCR models (Schofield et al., 2018). We then consider separately the process for marks (eg, animal identity, detection location, and

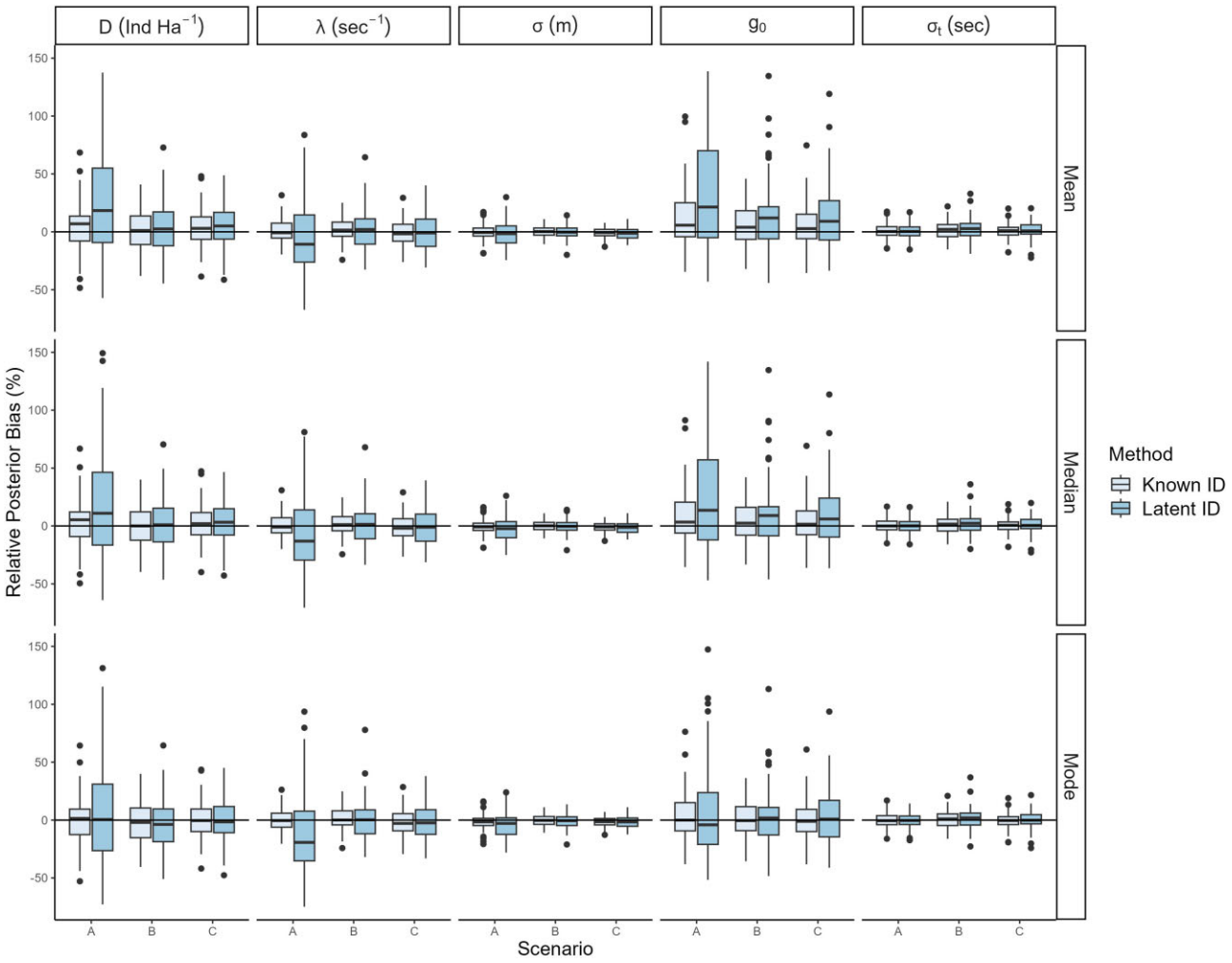

FIGURE 5 Acoustic spatial capture-recapture posterior relative bias for 2 different ASCR models: known ID and Latent ID. D is animal density, λ is the cue rate, σ is the scale parameter, g_0 is the probability of a cue being recorded at distance 0 from the microphone, and σ_t is the standard error of the time of arrival. Relative posterior bias is shown for each point estimate. The y-axis is cut-off at 150% bias, which removed 4 simulated datasets from scenario A with latent ID. Scenarios are $\sigma_t =$ (A) 0.05, (B) 0.001, and (C) 0.00055. Abbreviation: ASCR, acoustic SCR.

sex) making it easy to extend known ID SCR models to LID-SCR models within the same framework.

When the identity mark is unobserved, the MPP formulation naturally becomes a mixture model. This includes the special case of the SC model from Chandler and Royle (2013), but also by incorporating partially identifying covariate information includes SPIM models (Augustine et al., 2018; 2019), and spatial mark-resight (Whittington et al., 2018) models. Our methods highlight that these models only differ in the amount of the mark information available (Sun et al., 2022). Augustine et al. (2019) applied their model to a genetic hair snag study where they assumed a Bernoulli data generation process. In our framework, the total counting process per detector becomes a Poisson binomial distribution, and we can continue to apply the methods described here.

Another advantage of our formulation is that it does not require custom code to be written for the various models that fall in the framework, but instead requires just simple adaptations of the general code template. The fisher example highlights this by requiring minimal changes to the model and MCMC sampler to incorporate different mark types. The sex mark shows how an animal feature that is associated with each individual can be incorporated even when not fully observed. Inclusion of the collar mark shows how very study-specific information may be included. In this case, the collars were partially identifying characteristics that changed over time, which would normally be challenging to incorporate but could be readily included in our framework. Our frog example demonstrates the framework's flexibility by using it to solve a latent ID-ASCR problem, which has not been tackled in previous literature.

Similar to other studies, we found that estimating animal density from camera trap data without animal identities is too imprecise to be useful (Burgar et al., 2018; Amburgey et al., 2021; Doran-Myers et al., 2021). However, with additional information from available marks, such as sex, collar, and TOA in the case of acoustic detectors, we were able to obtain practically useful estimates. This was true even when the additional marks were only partially observed. We recommend caution when applying these methods without additional mark information, and to design surveys with this in mind.

We have presented a framework for dealing with LID-SCR surveys using a marked point process. Our methods apply to SCR-type surveys using passive detectors, where individuals may not be fully identifiable. They also apply to to both SC and SPIM type problems and, thus, can be used for existing applications of LID-SCR. By coding all models in Nimble, we provide a readily customizable, user-friendly implementation of the methods and make it easy to extend these further.

ACKNOWLEDGMENTS

The authors thank Ben Augustine for the useful discussions about this manuscript. We acknowledge the funding support of the Natural Sciences and Engineering Research Council of Canada (NSERC), the University of St Andrews, and the Royal Society of New Zealand.

SUPPLEMENTARY MATERIALS

Supplementary material is available at *Biometrics* online.

Web Appendices, Tables, and Figures referenced in Sections 4.1, 5.1, and 5.2 and data and code referenced in Sections 4.1 are available with this paper at the Biometrics website on Oxford Academic.

FUNDING

The fisher study was funded by InnoTech Alberta grants, the Government of Alberta (Environment and Parks), the Beaver Hills Initiative, Alberta Conservation Association, NSERC, Royal Canadian Geographic Society, TD Friends of the Environment Foundation, and the Fur Institute of Canada scholarships.

CONFLICT OF INTEREST

None declared.

DATA AVAILABILITY

The data used in this manuscript are available in a Github repository {https://github.com/paul-vdb/latentIDPaper} as well as in the Web Appendix.

REFERENCES

Alonso, R. S., McClintock, B. T., Lyren, L. M., Boydston, E. E. and Crooks, K. R. (2015). Mark-recapture and mark-resight methods for estimating abundance with remote cameras: a carnivore case study. *PloS One*, 10, e0123032.

Amburgey, S. M., Yackel Adams, A. A., Gardner, B., Hostetter, N. J., Siers, S. R., McClintock, B. T. et al. (2021). Evaluation of camera trap-based abundance estimators for unmarked populations. *Ecological Applications*, 31, e02410.

Augustine, B. C., Royle, J. A., Kelly, M. J., Satter, C., Alonso, R. S., Boydston, E. E. et al. (2018). Spatial capture–recapture with partial identity: an application to camera traps. *The Annals of Applied Statistics*, 12, 67–95.

Augustine, B. C., Royle, J. A., Murphy, S. M., Chandler, R. B., Cox, J. J. and Kelly, M. J. (2019). Spatial capture–recapture for categorically marked populations with an application to genetic capture–recapture. *Ecosphere*, 10, e02627.

Borchers, D., Distiller, G., Foster, R., Harmsen, B. and Milazzo, L. (2014). Continuous-time spatially explicit capture–recapture models, with an application to a jaguar camera-trap survey. *Methods in Ecology and Evolution*, 5, 656–665.

Borchers, D. L. and Efford, M. G. (2008). Spatially explicit maximum likelihood methods for capture–recapture studies. *Biometrics*, 64, 377–385.

Borchers, D. L., Stevenson, B. C., Kidney, D., Thomas, L. and Marques, T. A. (2015). A unifying model for capture–recapture and distance sampling surveys of wildlife populations. *Journal of the American Statistical Association*, 110, 195–204.

Burgar, J. M., Stewart, F. E., Volpe, J. P., Fisher, J. T. and Burton, A. C. (2018). Estimating density for species conservation: Comparing camera trap spatial count models to genetic spatial capture–recapture models. *Global Ecology and Conservation*, 15, e00411.

Chandler, R. B. and Royle, J. A. (2013). Spatially explicit models for inference about density in unmarked or partially marked populations. *The Annals of Applied Statistics*, 7, 936–954.

Cowen, L. L., Besbeas, P., Morgan, B. J. and Schwarz, C. J. (2017). Hidden Markov models for extended batch data. *Biometrics*, 73, 1321–1331.

Daley, D. J. and Vere-Jones, D. (2003). *An Introduction to the Theory of Point Processes: Volume I: Elementary Theory and Methods*. Springer: New York.

Dawson, D. K. and Efford, M. G. (2009). Bird population density estimated from acoustic signals. *Journal of Applied Ecology*, 46, 1201–1209.

de Valpine, P., Paciorek, C., Turek, D., Michaud, N., Anderson-Bergman, C., Obermeyer, F. et al. (2020). NIMBLE user manual. R package manual version 0.9.1.

de Valpine, P., Turek, D., Paciorek, C., Anderson-Bergman, C., Temple Lang, D. and Bodik, R. (2017). Programming with models: writing statistical algorithms for general model structures with NIMBLE. *Journal of Computational and Graphical Statistics*, 26, 403–413.

Doran-Myers, D., Kenney, A., Krebs, C., Lamb, C., Menzies, A., Murray, D. et al. (2021). Density estimates for Canada lynx vary among estimation methods. *Ecosphere*, 12, e03774.

Efford, M. (2004) Density estimation in live-trapping studies. *Oikos*, 106, 598–610.

Haario, H., Saksman, E. and Tamminen, J. (2001). An adaptive Metropolis algorithm. *Bernoulli*, 7, 223–242.

Jasra, A., Holmes, C. C. and Stephens, D. A. (2005). Markov chain Monte Carlo methods and the label switching problem in Bayesian mixture modeling. *Statistical Science*, 20, 50–67.

Jiménez, J., Augustine, B. C., Linden, D. W., Chandler, R. B. and Royle, A. J. (2021). Spatial capture–recapture with random thinning for unidentified encounters. *Ecology and Evolution*, 11, 1187–1198.

Linden, D. W., Fuller, A. K., Royle, J. A. and Hare, M. P. (2017). Examining the occupancy–density relationship for a low-density carnivore. *Journal of Applied Ecology*, 54, 2043–2052.

Link, W. A. (2013) A cautionary note on the discrete uniform prior for the binomial N. *Ecology*, 94, 2173–2179.

McClintock, B. T., Abrahms, B., Chandler, R. B., Conn, P. B., Converse, S. J., Emmet, R. L. et al. (2022). An integrated path for spatial capture–recapture and animal movement modeling. *Ecology*, 103, e3473.

Measey, G. J., Stevenson, B. C., Scott, T., Altwegg, R. and Borchers, D. L. (2017). Counting chirps: acoustic monitoring of cryptic frogs. *Journal of Applied Ecology*, 54, 894–902.

Neal, R. M. (2003). Slice sampling. *The Annals of Statistics*, 31, 705–767.

R Core Team. (2019). *R: A Language and Environment for Statistical Computing*. Vienna, Austria: R Foundation for Statistical Computing.

Rich, L. N., Kelly, M. J., Sollmann, R., Noss, A. J., Maffei, L., Arispe, R. L. et al. (2014). Comparing capture–recapture, mark-resight, and spatial mark-resight models for estimating puma densities via camera traps. *Journal of Mammalogy*, 95, 382–391.

Royle, J. A., Chandler, R. B., Sollmann, R. and Gardner, B. (2013). *Spatial Capture–Recapture*. Amsterdam: Academic Press.

Royle, J. A. and Dorazio, R. M. (2012). Parameter-expanded data augmentation for Bayesian analysis of capture–recapture models. *Journal of Ornithology*, 152, 521–537.

Rushing, C. S. (2023). An ecologist's introduction to continuous-time multi-state models for capture–recapture data. *Journal of Animal Ecology*, 92, 936–944.
Schofield, M. R., Barker, R. J. and Gelling, N. (2018). Continuous-time capture–recapture in closed populations. *Biometrics*, 74, 626–635.
Sollmann, R., Gardner, B., Parsons, A. W., Stocking, J. J., McClintock, B. T., Simons, T. R. et al. (2013). A spatial mark–resight model augmented with telemetry data. *Ecology*, 94, 553–559.
Stevenson, B. and Borchers, D. L. (2018). *ascr: Acoustic Spatial Capture–Recapture*. R package version 2.2.4.
Stevenson, B. C., Borchers, D. L., Altwegg, R., Swift, R. J., Gillespie, D. M. and Measey, G. J. (2015). A general framework for animal density estimation from acoustic detections across a fixed microphone array. *Methods in Ecology and Evolution*, 6, 38–48.
Stevenson, B. C., van Dam-Bates, P., Young, C. K. and Measey, J. (2021). A spatial capture–recapture model to estimate call rate and population density from passive acoustic surveys. *Methods in Ecology and Evolution*, 12, 432–442.
Stewart, F. E., Darlington, S., Volpe, J. P., McAdie, M. and Fisher, J. T. (2019). Corridors best facilitate functional connectivity across a protected area network. *Scientific Reports*, 9, 10852.
Stewart, F. E., Volpe, J. P., Taylor, J. S., Bowman, J., Thomas, P. J., Pybus, M. J. et al. (2017). Distinguishing reintroduction from recolonization with genetic testing. *Biological Conservation*, 214, 242–249.
Sun, C., Burgar, J. M., Fisher, J. T. and Burton, A. C. (2022). A cautionary tale comparing spatial count and partial identity models for estimating densities of threatened and unmarked populations. *Global Ecology and Conservation*, 38, e02268.
Tanner, M.A. and Wong, W.H. (1987). The calculation of posterior distributions by data augmentation. *Journal of the American Statistical Association*, 82, 528–540.
Turek, D., Milleret, C., Ergon, T., Brøseth, H., Dupont, P., Bischof, R. et al. (2021). Efficient estimation of large-scale spatial capture–recapture models. *Ecosphere*, 12, e03385.
Whittington, J., Hebblewhite, M. and Chandler, R. B. (2018). Generalized spatial mark–resight models with an application to grizzly bears. *Journal of Applied Ecology*, 55, 157–168.

Received: November 18, 2022; Revised: October 30, 2023; Accepted: November 22, 2023